

Tutorial

Practical aspects of modern interferometry for optical manufacturing quality control: Part 2

Robert Smythe

R.A. Smythe, LLC, 439 Higby Rd., Middletown, CT 06457, USA

e-mail: Robert@RASmythe.com

Received April 30, 2012; accepted June 13, 2012

Abstract

Modern phase shifting interferometers enable the manufacture of optical systems that drive the global economy. Semiconductor chips, solid-state cameras, cell phone cameras, infrared imaging systems, space based satellite imaging and DVD and Blu-Ray disks are all enabled by phase shifting interferometers. Theoretical treatments of data analysis and instrument design advance the technology but often are not helpful towards the practical use of interferometers. An understanding of the parameters that drive system performance is critical to produce useful results. Any interferometer will produce a data map and results; this paper, in three parts, reviews some of the key issues to minimize error sources in that data and provide a valid measurement.

Keywords: Fizeau; interferometer; measurand; reference surface; Twyman-Green.

1. Introduction to part two

Interferometers are enabling tools in high-technology manufacturing. Therefore, a practical understanding of interferometry, its application and sense of future direction is required in the field of optics. This paper will focus on those aspects in three parts. Part 1 [1] covered the history and basic descriptions of interferometer systems, this section, part 2, covers test configurations, data acquisition and metrology, and part 3 will cover advance techniques, software and future directions.

It is very easy to acquire highly repeatable results with modern interferometers. Achieving results with low measurement uncertainty requires knowledge of data acquisition techniques and an understanding of the limiting errors present in a test set-up. This section will introduce the basic concepts of the most common data acquisition techniques and then reviews metrology concepts, problems and solutions encountered in optical shop testing.

2. Interferometer test configurations

Laser Fizeau and Laser Twyman-Green interferometers (referred to as a Fizeau and T-G herein), are the most common systems used in optical testing [2]. These systems are very flexible and can be configured to measure flat, prismatic, spherical, cylindrical, conical and aspheric surfaces, plus finite or infinite conjugate tests of optical system wavefront.

Common test configurations are presented in Table 1 [3, 4].

2.1. Modularity enables flexibility

Commercial interferometers perform multiple tests from a set of standard modules. References in the following list of modules refer to Table 1 as examples of where they are used.

2.1.1. Illumination, imaging The ‘mainframe’, ‘head’ or ‘interferometer’ (shown only in 1A but is assumed present in all other configurations). It outputs a collimated wavefront and produces a variable magnification image with focus control of the return wavefront.

2.1.2. Data acquisition Computer and software (not shown) to control data acquisition, analysis and display. This module will be discussed in Part 3 of this paper.

2.1.3. Focusing optics Transforms the collimated wavefront into a spherical wavefront (D, E, F, G, H, I, J).

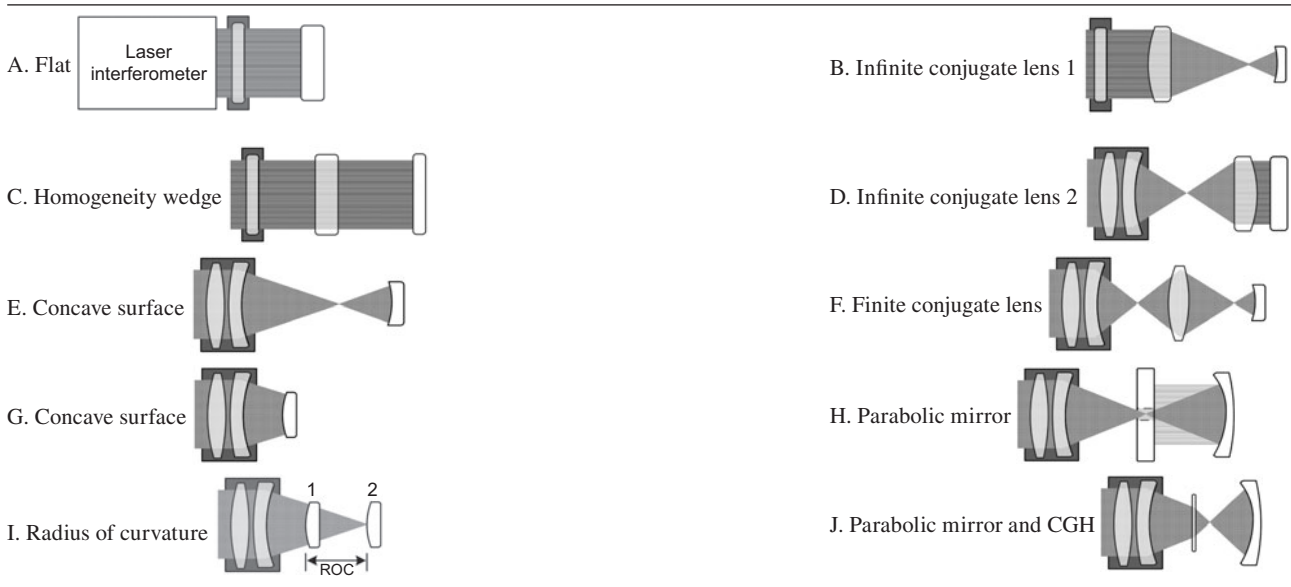
2.1.4. Reference surface For a T-G the reference surface is located inside the mainframe. The Fizeau reference is the part side surface of reference flat, the first element (A, B, C) or last surface (part side) of the focusing lens (D, E, F, G, H, I, J). The flat reference is also called a ‘transmission flat or TF’. The focusing optic is also called a ‘Fizeau lens, transmission sphere or TS’.

2.2. Radius of curvature optical bench

Combines a linear slide with laser or glass scales to position the test surface at the catseye and confocal positions to measure radius of curvature (I, convex part shown).

2.3. Null lens

Transforms the collimated or spherical wavefront into an aspheric wavefront to measure aspheric surfaces. Null lenses can be a lens system or computer generated hologram or CGH (J).

Table 1 Common interferometer test configurations.

2.4. Plane parallel transparent plates

Transparent parts with plane parallel surfaces are an important subclass with special testing issues. These parts are used for filters, windows, substrates for magnetic disks and high brightness light emitting diodes. The plane parallel surfaces produce internal Fizeau fringes that confuse the interferometer data acquisition system. Several approaches are used to measure these parts. The simplest is coating the back surface with grease, gel or paint to suppress the back surface reflections, thus minimizing internal Fizeau interference. An index matching fluid can also be used. But none of these approaches is applicable to production. Several interferometer designs eliminate this problem. Their main approach is the control of the illumination coherence to prevent the formation of internal Fizeau fringes [5–8].

2.5. Asphere surfaces

Asphere metrology is one of the fastest growing areas of interferometric testing. The measurement requirements can be separated into axially symmetric form such as spherical aberration, non-axially symmetric form such as astigmatism and mid-spatial frequency errors. Aspheric form has been primarily measured using stylus profilers and coordinate measuring machines (CMMs) [9–11]. These typically measure the axially symmetric form errors and some mid-spatial frequencies along one line. Interferometers have been used to measure the non-axially symmetric form and higher spatial frequencies of waviness using null lenses and CGHs as shown in Table 1J [12, 13]. With the addition of accurate radius of curvature measurement interferometers are now able to measure asphere form to comparable measurement uncertainty of stylus profiler or CMMs in commercial situations as discussed

below and with much higher accuracies in specialized applications [14]. Three approaches are currently being used for asphere surface measurement with interferometry: stitching, scanning and sub-nyquist metrology.

Surface slope acceptance limits interferometric measurement of aspheres. As the slope of the spherical reference to aspherical test wavefront increases more interference fringes are produced. When the fringe density exceeds the imaging system nyquist frequency [15] measurement fails. To extend the slope measurement range, interferometers either overcome the nyquist limit or limit the measured area on the surface to maximize slope acceptance.

Stitching interferometry limits the area measured and stitches the surface together [16]. This has multiple benefits. Slope is only limited by how many patches can be measured and the time allowed. The many measurements improve the reference wavefront uncertainty through averaging, and high-resolution data (1 000 000 pixels) is acquired. When radius of curvature is also measured stitching has demonstrated form measurement uncertainty of <50 nm.

Scanning interferometry limits the area measured to rings and creates a cloud of points of the surface [17, 18]. Scanning interferometry requires an integrated radius of curvature measurement. The system moves to the expected radius position for the ring to be measured, any deviation in the ring position is an error in the surface. This methodology minimizes ray-mapping errors (see section 5 below) and errors due to image distortion. Scanning interferometry cannot measure non-axially symmetric surfaces, a major limitation. High-resolution data (1 000 000 pixels) is acquired. Scanning interferometry has produced <10 nm form measurement uncertainty.

Sub-nyquist interferometer extends the slope acceptance by masking the camera [19]. At the nyquist frequency fringe contrast is zero. By masking each camera pixel to a smaller

size the fringe contrast is increased. Now data acquisition is possible. The analysis software is able report surface shape with *a priori* knowledge of the expected shape. With a measurement of radius of curvature sub-nyquist can measure form plus higher order aberrations, without radius of curvature measurement sub-nyquist is equivalent to an infinite flexibility CGH or null lens. A major benefit is non-axially symmetric form, such as torics, is measurable [20]. High-resolution data (250 000 pixels) is typically acquired.

Optical surfaces for cell phone camera lenses and other imaging optics have reversing curvatures. These surfaces, called sombrero or gull-wing surfaces due to the shapes of the profiler traces, are not measurable by interferometers. This is the major reason interferometers have yet to replace contact probes for asphere measurement. As asphere optics migrate to free form shapes, interferometry will be further challenged.

3. Data acquisition techniques

The mini and personal computer eras, combined with the laser, launched modern interferometry by enabling phase measuring data acquisition. Prior to computerized phase measurement surface form was determined visually by assessing the straightness of the fringes. Sensitivity was approximately 30 nm and operator-to-operator error up to 120 nm. The combination of computers, cameras and in some cases precision mechanics allowed multiple intensity patterns to be analyzed for phase [21]. Phase measurement is sensitive to many thousands of a fringe, and more importantly is operator-independent, repeatable metrology. There are two classes of phase measurement acquisition: time varying or phase shifting interferometry (PSI) and simultaneous PMI (SPMI), sometimes called instantaneous PMI (IPMI).

3.1. Temporal methods: phase shifting interferometry (PSI)

PSI is the most common data acquisition technique and measures multiple cavity phases over time. Typically, the distance between the reference and test surfaces is changed to modulate the interferometer phase [22, 23], although other phase modulation techniques are possible [24, 25].

PSI has many benefits in addition to higher fractional fringe resolution. Each camera pixel acquires data independently; therefore, the image resolution nominally equals the number of camera pixels that are illuminated. Higher image resolution is important for process control of spot polishing techniques [26]. Modern cameras provide over a megapixel of data in some cases. Furthermore, independent pixel acquisition eliminates the effects of pixel-to-pixel sensitivity variations.

Numerous PSI data acquisition algorithms exist with various advantages and are summarized elsewhere [27]. Data acquisition algorithms minimize the effects of non-linearity and calibration errors of the phase shifting mechanism, and vibration and air turbulence in the cavity. Recent developments in PSI algorithms are providing vibration and air turbulence insensitivity approaching SPMI [28].

3.2. Spatial methods: simultaneous phase measuring interferometry (SPMI)

SPMI measures all the phases at the same time by separating the phases spatially. Whereas time varying errors affect PSI, spatial varying errors affect SPMI. There are three primary SPMI data acquisition methods: displaced image, carrier fringe and direct measuring interferometry.

Displaced image utilizes multiple images of the test object, each phase shifted by a known amount, typically $\pi/2$ [29]. These images are then combined with standard PSI algorithms to produce phase at each 'pixel'. Each pixel phase is the combination of multiple pixel intensities from displaced images. The multiple phase-shifted images are created using polarization techniques; polarization 'encodes' the test and reference signal. One implementation uses a T-G interferometer where a polarization beamsplitter sends the S polarization to the reference and the P polarization to the test arm. The use of a quarter wave plates recombines the beams into the imaging arm while maintaining their encoding [30]. Several Fizeau configurations have been demonstrated. In each configuration the Fizeau cavity is polarization encoded. To achieve this encoding the illumination beam is given a slight angular shift [31] or a secondary cavity is created utilizing low coherence illumination [32, 33].

The encoded test and reference beams are phase shifted with respect to each other via one-half and a quarter waveplates or equivalents. The images are either analyzed as whole images on multiple cameras [34], multiple images on one camera, or as 'super pixels' where each 2×2 array of pixels contains the four phase shifted intensity data [35]. It is important to note that multiple pixels, typically four, are required to acquire phase data. Therefore, in the 'super pixel' configuration a 1000×1000 pixel camera will acquire data that is equivalent to a 512×512 pixel camera using PSI [36].

Carrier fringe and direct measuring interferometry appear similar to the user, but utilize different data analysis algorithms with different 'filtering' functions. Direct measuring interferometry introduces tilt fringes in the interferometer until each pixel is phase shifted by $\pi/2$ relative to its neighbors. Phase is measured at each pixel via a 3×3 super pixel that is convolved with a complex-valued convolution kernel [37]. Carrier fringe also introduces tilt fringes and then extracts phase via a Fourier analysis over the entire image, whereby the intensity data are removed and phase data are displayed via filtering in phase space [38].

The two methods are different regarding how the spatial data are 'filtered'. For the direct measuring method the spatial region that influences the phase value at each pixel is limited by the size of the convolution kernel. Therefore, the 'filtering' behavior is homogeneous across the whole interferogram as determined by the size of the super pixel. Whereas in the carrier fringe method the effective region that influences the phase value of any pixel varies across the aperture and this area is much larger than that of direct measuring interferometry.

In all three approaches multiple pixels acquire data. Displaced images and carrier fringe have been shown to exhibit functionally equivalent image resolution for equally

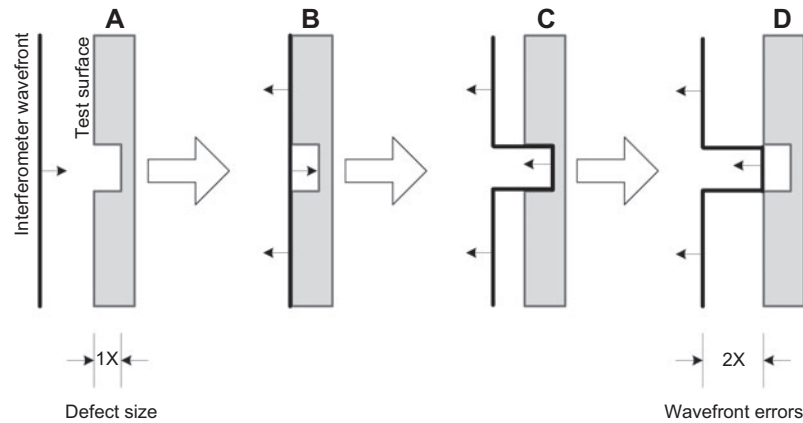


Figure 1 Interferometer sensitivity.

dense pixel or super pixel arrays [39]. When compared to PSI data acquisition, SPMI produces approximately one-fourth the data density per equivalent pixel imager.

In all of SPMI cases the reference and test are spatially shifted either by inducing tilts, or separate test and reference paths. These additional tilts and paths cause errors to accumulate in the interferometer. What is gained in techniques to minimize environmental induced errors is compromised with interferometer-induced errors. As with most errors calibration is required to minimize their effects. As care must be taken to minimize the effects of vibration and air-turbulence in PSI, interferometer wavefront errors must be calibrated to minimize their effects in SPMI. When properly calibrated SPMI interferometers fully rival PSI systems in measurement uncertainty.

4. Metrology

Interferometers are used for process control. Modern interferometers are relatively easy to use, very repeatable and produce beautiful high-density data maps. It is easy to assume they are producing sufficient measurement uncertainty from such powerful tools. Yet process control demands the metrology be better than the process to be controlled. The measurement quality depends on the operator requesting the right parameters, optimizing the test set-up, calibrating as required and controlling the environment. This is especially important as surface quality exceeds 50 nm PV, a common specification today.

There are many test configurations as described in section 3, yet optimizing the interferometer performance has common themes regarding minimizing measurement uncertainty [40]. Those common themes will be explored.

4.1. Measurand [41]

What is being measured? This simple question is often assumed and needs careful consideration. The following are a list of questions to ask with example answers:

What results are desired? PV, RMS, power spectral density, slope...

What is the clear aperture? Can the edge be excluded, if so how much?

What image resolution is required? >50 000 points or 800 000 points?

Is filtering to be applied? Low pass filter or Zernike polynomials and if so to what order?

Does the user require form data separated from mid-spatial frequencies? How?

What temperature or temperature range is the part to be tested at?

Is the part used horizontally or vertically or both?

Does test wavelength matter?

What will the measurement be used for? Form qualification? Polishing machine feedback?

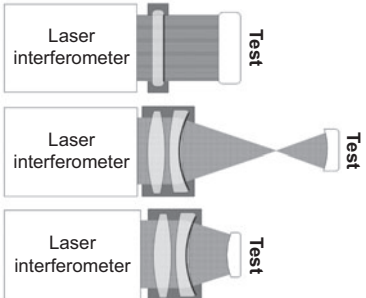
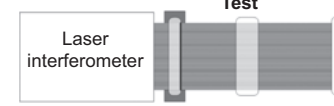
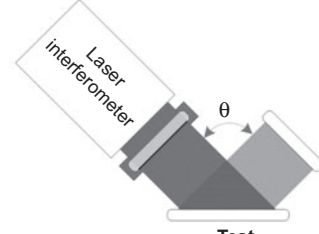
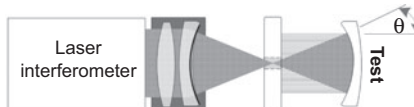
When disagreements between measurements arise, especially between manufacturer and user, the measurand is the best place to start to confirm both parties are reporting the same data.

4.2. Interferometer sensitivity

Interferometers measure optical wavefronts based on the wavelength of light. The interferometer sensitivity depends on the test configuration. The sensitivity of a particular test configuration is the ratio of the resulting wavefront deviation to the given surface height deviation (both measured in units of the wavelength). Figure 1 shows the case where a surface is touched by the probing wavefront only once; this is called single pass.

For single pass and normal incidence we have a sensitivity of 2, that is, the wavefront deviation that is imprinted by the surface profile of the part onto the wavefront becomes twice as large, refer to Table 2, cases A and B. This can be understood when looking at Figure 1 at the third 'frame' of this symbolic time lapsed sequence of the wavefront in flight: when the central part of the wavefront has reached the bottom of the center groove, the outer parts have been already reflected and travelled back by twice the steepness of the groove. The more general case

Table 2 Sensitivity factor.

Case	Description	Test configuration	Sensitivity
A	Single pass for flat and spherical surfaces		2
B	Double pass window		
C	Double pass @ angle θ for flat surface test		$4 \cdot \cos(\theta)$
D	Double pass @ varying angle θ for parabolic surface test		

considers the angle of incidence and reflection; for any angle θ the single pass sensitivity becomes $2 \cdot \cos(\theta)$. Note: there are test configurations where the incident and reflection angle varies across the test part. Table 2, case D shows such a case testing a parabolic mirror with an autocollimation flat with a central hole.

In double- or multiple-pass configurations the surface is probed twice or multiple times by the wavefront, for example Table 2 case C, thus increasing the sensitivity of the set-up. There are drawbacks to the increased sensitivity. When multiple passes are used the test surface is imaged at two different focus positions. It is impossible to focus on both images at the same time and one image will be out of focus. Depending on the optical configuration the higher spatial frequencies may be measured falsely. Refer also to Table 3X.

To correct for the variations in fringe sensitivity the analysis software provides an input parameter often termed 'scale factor'. Scale factor is calculated as inverse sensitivity ($1/\text{sensitivity}$). This input corrects the calculated results to match the test configuration. It is highly recommended that the user refers to each particular software program regarding how this parameter is handled.

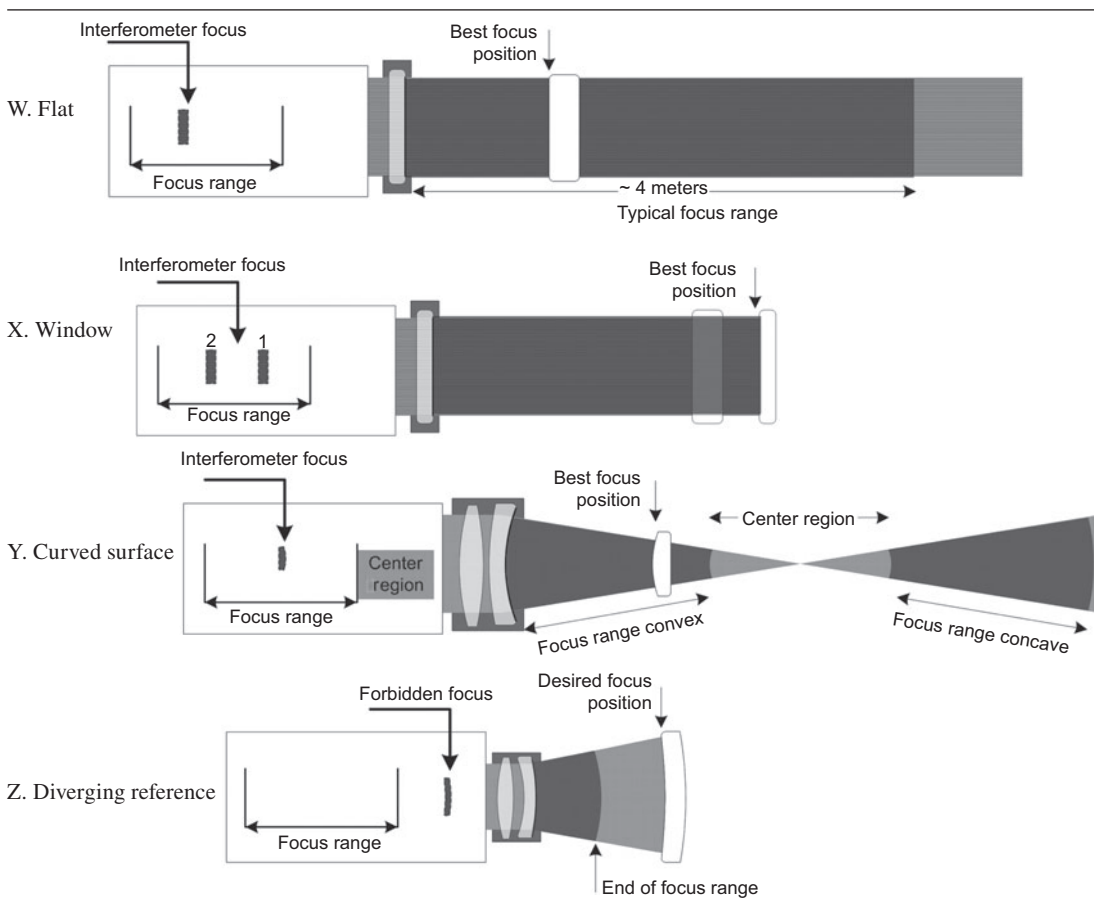
4.3. Sources of error

Error sources are both systematic (static) and random (dynamic, i.e., time varying). First random errors will be addressed.

Random errors are always present and typical random errors are vibration and air turbulence. In principle averaging can minimize random errors, but the amplitude and frequency of these errors determine the effectiveness of averaging and what data acquisition system is most appropriate to use.

Slowly varying random errors are difficult to minimize by averaging. Consider a test cavity where air turbulent disturbs the cavity by 96 nm PV every 5 s. If 60 nm PV surface quality is required, a measurement repeatability of 6 nm is a typical goal. Averaging improves the repeatability by the square root of the number of averages of n cycles of the 'varying parameter', not n data acquisitions. In this case to achieve 6 nm repeatability, 256 cycles of air turbulence must be covered during the measurement sequence or 21 min of data acquisition.

A common error is to completely enclose the measurement cavity to minimize turbulence. Repeatability improves, but now thermal gradients induce static or very slowly varying random errors that cannot be removed. Adding turbulence plus averaging produces more consistent metrology results. When the amplitudes of the turbulence or vibration are >150 nm, such as in a test tower, standard PSI data acquisition will fail. Data acquisition can be achieved with SPMI to 'freeze' wildly moving fringes, thus allowing data averaging to minimize these random errors. Data acquisitions >12 h are possible and sometimes required in these cases.

Table 3 Focus range and position for various cavity configurations.

Observing the range of values taken over several minutes for a measured parameter can approximate random errors. Observing the rate this range decreases with averaging indicates how much averaging is required to achieve acceptable metrology results.

4.4. Systematic errors

Systematic errors can be invisible. Calibration and measurement techniques are required to minimize these errors. Systematic errors can be approximated by comparing the results of measuring the same part on multiple instruments, or observing the reproducibility of 'absolute' measurements (see below) on one instrument.

The primary source of systematic errors in a Fizeau is the reference surface, and in the T-G the reference surface, beam-splitter and focus lens assembly. For simplicity the Fizeau will primarily be discussed. The calibration techniques apply to both systems.

Standard manufacturing tolerances for reference flats are 32 nm PV ($\lambda/20$) and for reference spheres 64 nm PV ($\lambda/10$). A flat reference can exhibit 32 nm PV of power and higher order aberrations within specification. When compared to another reference flat whose errors can be of the opposite

sign, the resulting cavity power will be ≤ 64 nm PV. A spherical reference surface can contain low order aberrations, such as astigmatism and coma of up to 63 nm PV. Therefore, a test part measured using two separate reference spheres could have PV values that differ by ≤ 126 nm. When a vendor and supplier are testing the same part these potential discrepancies need to be considered during part acceptance [42].

Reference accessories are designed for thermal stability, but over a limited range, often not published. When testing at temperatures deviating by $\pm 2^\circ\text{C}$ from 20°C , it is assumed that thermal effects degrade performance. Thermal effects are a major source of systematic errors in a T-G due to the complexity of the interferometer path. Calibration plus thermal stability minimizes this issue.

Testing in a vertical configuration induces gravitational bending to the reference optic and potentially in the test optic. In this configuration the reference is horizontal and bends downward in the middle under gravitational pull. Circular plate stiffness increases as the third power of thickness, while weight increases linearly with thickness. Therefore, increasing the reference plate thickness is a practical method to decrease gravitational bending. Bending also increases with the fourth power of part radius. Therefore, large diameter parts become much more problematic, especially thin lenses

where it is impossible to adequately minimize bending. Well-designed mounting structures with three points or multipoint seesaw systems are necessary, plus mathematical modeling to calculate and remove residual bending from the reported results. Again thin large diameter parts are very difficult to measure without gravitation bending errors.

4.5. Calibration

The simplest calibration is a 'gold' standard. A 'gold standard' is typically higher quality than the target tolerance, is thermally stable, well characterized and similar to the parts to be tested. When the part is measured any deviation from perfection is assumed to be systematic error. This 'error map' is stored in the computer and subtracted from future data sets. The gold standard is excellent for use in production to improve system-to-system correlation by minimizing systematic errors and correcting long period random errors such as thermal variations.

An extension of the gold standard is the calibration ball [43]. The calibration ball is a precision manufactured sphere that is used for multiple measurements. Between each measurement the ball is rotated and the measurements are averaged together. The benefit is that surface and random measurement errors are reduced by the square root of the number of averages producing a high quality error map of the reference surface, as the average of the ball surface errors can be assumed to be zero.

The most accurate method of calibration is the absolute measurement. Absolute measurement techniques isolate the measured surfaces without influence of the other surfaces used in the test. The classical three-flat [44, 45] and two-sphere [46] tests are absolute tests. They measure several similar parts and mathematically extract each individual surface. The two-sphere test produces a map of the entire surface, whereas the classic three-flat test only produces a horizontal and vertical profile across the surface. Different attempts have been published to improve the test including separating of rotationally symmetric and rotationally varying error terms [47, 48]. If one of the surfaces is the reference surface the surface map can be used as the error map. Finally, reproducibility of these tests indicates that errors are due to the set-up and therefore is a good indication of limits of measurement within a particular environment, operator or set of procedures.

4.6. Cavity alignment

Cavity alignment is critical to minimize systematic errors. The reference surface must first be aligned perpendicular to the measurement axis. Modern interferometers have alignment modes where the reference surface can be nominally aligned on axis. This is not sufficient for quality metrology. For Fizeau reference flats or collimated T-G, a corner cube retro reflector is used as the test part and the reference tilted until the return fringes are nulled. To align a reference sphere (Fizeau) or focusing optic (T-G), place a flat at the catseye position (where the focus returns on itself). Adjust to minimize the focus error, by minimizing the power fringes, and

then for a Fizeau, tilt the reference sphere to balance the tilt term in x and y. For a T-G, adjust the focusing optic to minimize aberrations. An alternative approach for the T-G is to place a corner cube retro reflector in the reference arm (if accessible) and placing a flat mirror on the face of the focusing lens, and then adjusting the focus lens to minimize tilt in the cavity. In all cases, use of the data acquisition system to measure tilt and aberrations provides the greatest sensitivity. Now the cavity is on axis.

4.7. Part alignment

T-G and Fizeau interferometers are designed to work on-axis. Just as the reference optics must be aligned, the test part must also be aligned. It is not uncommon for users to align a part with two to four fringes of tilt and then to acquire the data. This tilt introduces a slope error in the return optics, introducing a ray-mapping or ray-tracing error. The sensitivity of this alignment depends on the particular interferometer. An estimate of the alignment errors is possible by acquiring data with minimal tilt (null fringes) storing this data as a 'reference' and then systematically adding tilt while subtracting the 'reference' data. This will quantify the magnitude of this error. The user can then align the optics appropriately to the target tolerance. Best practice is to always align the part, that is, null the fringes.

For flats and spherical parts it is possible to minimize these errors. As parts deviate from a sphere or flat it is impossible to adjust these local slope errors out of the measurement. Interferometers are designed to operate on-axis, as the part approaches spherical the errors reduce. This is not true for aspheres and the systems mentioned earlier are designed to minimize or compensate for these ray-mapping errors.

4.8. Part mounting

Part mounting can degrade the measurement. Convenient 'three point adjustable mounts' are available from many manufacturers. They center the part approximately at the correct height and provide tip and tilt adjustment. The mount exerts pressure at the three mounting points. For thin optics the pressure can warp the optic. Warping is observed by a triangular pattern in the data that remains fixed as the part is rotated. Even more insidious is the warping and deflection of vertically mounted large optics that rest on two pins. Its weight deforms the optic at the point of contact and is a fixed error. Mathematical removal of this deformation is required [49]. Previously discussed was gravitational warping of horizontal flats.

There are several strategies to hold large optics for horizontal testing. The best approaches deterministically spread the loading around the part to minimize deformation. A soft ring (foam) can be placed under the part, but can complicate phase measurement. Single- or multiple-independent narrow flexible bands around the part have also been used effectively. Finally, three or six point seesaw mounts spread the loading while controlling the points of contact and simplifying phase measurement and part adjustment control.

4.9. Focus

Focusing on the part is important to maximize the measured surface detail and also to minimize the degrading effects of diffraction on edges and artifacts. Focusing appears as a very easy concept, except in an interferometer the imaging is coherent and phase is the parameter being measured. This complicates the role of focusing greatly and very little has been written about focus and interferometer design. Several partial coherent illumination designs will be discussed in part 3 of this paper that minimize coherent imaging errors.

Focus range and best focus position depend on the cavity set-up. Table 3 identifies four representative cases. Both part position in the cavity and a representative image position within the interferometer are diagramed. The collimated test cavity (case W) typically has a focus range of 4 m. The best focus in case W is at the test surface as expected. For a window measurement (case X) the imaging system sees two images of the window: once going out and once on return. It is best in this case to balance the focus at the return mirror and move the window as close to the return mirror as possible.

To measure a curved surface (case Y) the spherical reference has two focus ranges. They correspond to the 4-m focus range. This leaves a 'center region' where it is not possible to focus on the part and positioning inside this center region compromises interferometer performance. If a test part falls into this region a smaller spherical reference is required, along with an aperture reducer to match the smaller spherical reference. A simple rule is that the test part radius of curvature should be larger than 20% of the reference sphere output focal length.

In some cases the test part may have a long radius of curvature, driving the need for a diverger or converger reference (case Z). These lenses push the virtual focus or the near point focus inside the interferometer. In a standard configuration the interferometer might not be able to focus on the part, as it will be outside the focus range as shown. The manufacturer can correct this with a custom adjustment to the imaging system.

4.10. Illumination system back reflections

Back reflections within the interferometer and reference optics create unwanted ghost fringes. These most likely occur in the center of the field at the vertex of the collimation and spherical reference decollimation optics. The operator can do little to minimize these errors. A manufacturing strategy is to apply high quality anti-reflection coatings to the intervening optics to minimize the errors. One user strategy is to adjust the focus and observe if there is a focus position that enables a sharp focus on the test part and minimizes ghost reflections. The other approach is to use masking in the data analysis software and simply remove the offending pixels.

4.11. Diffraction: artifacts

Dust, scratches and edges all diffract light and create interference fringes. Often these defects are called 'artifacts'. These

can occur anywhere along the optical path, from illumination, through the reference optics, off the test part and back through the imaging system to the camera. Depending upon where they occur relative to the focus position they will create varying sized background fringes. These fringes may or may not be detected by the data acquisition system but all of them affect the background illumination in non-predictable ways. Experience indicates that as the artifact size grows the contrast decreases and therefore its influence on the signal-to-noise and phase error decreases. There are no known published data quantifying this observation.

Most manufacturers strive to provide clean systems with minimum dust and scratches. This includes the reference optics. Dust will gather on the exposed surfaces and regular cleaning is required to remove the dust. A trained technician should only perform this cleaning to prevent damaging the delicate surfaces. Over time dust will also accumulate inside the interferometer and maintenance by a trained technician is required to clean the system, typically on an annual basis.

When artifacts are seen it is recommended to locate the artifact and remove it, focus the system to find an acceptable focus where the artifacts influence is reduced or as a last resort remove the artifact by filtering or removing its influence via masking.

4.12. Focus/slope induced errors

Again interferometers are designed to work on-axis. As parts deviate from a perfect sphere or flat more slope occurs between the test and reference wavefronts and errors are induced by the optical system. A focus driven systematic error occurs across the detector. This error occurs because the test part image is curved and the detector is flat. As slopes increase due to increased test part aspheric shape, the combination of the focus error and the slopes between the reference and test beams at the camera induce an error [50]. This error is out of the control of the user but is important to understand when selecting a system to measure aspheres. Improved measurement performance in the presence of this error is another benefit of partial coherent illumination systems described in part 3 of this paper.

4.13. Fringe contrast: optimizing signal-to-noise

Interference fringe contrast effects measurement repeatability. Measurement repeatability and signal-to-noise are optimized when fringe contrast is greatest. Fringe contrast is maximized when the test and reference return beam amplitudes are balanced. Often this is not possible, particularly with Fizeau interferometers; in practice, maintaining a five-to-one ratio between test and reference return illumination produces sufficient measurement repeatability.

In a T-G interferometer if a polarized laser and polarized beamsplitter are used, a rotatable one-half waveplate can balance the return illumination for maximum fringe contrast. This arrangement is very flexible enabling the measurement of high-reflectivity mirrors to anti-reflection coated optics and is one of the advantages of a T-G interferometer configuration.

Fizeau interferometers balance the test and reference return beams by controlling the reference surface reflectivity or inserting an attenuator into the test arm of the interferometer. Reference surfaces specially coated to produce ~20% reflectivity create a five-to-one or better ratio for both high-reflectivity mirrors and 4% raw glass material [51]. These coatings are typically found on flat references and high F-number focusing optics. Low F-number focusing optics are difficult to manufacture and maintain sufficient reference quality. For testing a high reflector using a 4% reflectivity reference an attenuator such as a reflective pellicle beamsplitter or a fine mesh window screen have been used. Again for low F-number optics there can be insufficient space between the test and reference to place the attenuator. Therefore, a Fizeau interferometer can accommodate various reflectivity test parts, but there are limitations.

4.14. Finesse in Fizeau fringes

In a Fizeau interferometer multiple reflections between the test and reference can narrow the profile of the interference fringes. This distortion is called fringe finesse, and it introduces higher order errors into the measurement. Modern data acquisition algorithms can accommodate finesse in the fringes [52]. Some of the same strategies to balance fringe contrast minimize the finesse of interference fringes, such as coatings to balance the test and reference and test arm attenuators. Finesse is not found in T-G systems.

4.15. Image distortion

Image distortion has two sources: in the imaging system and the reference sphere. Commercial interferometer imaging systems can exhibit classical barrel and pincushion distortion of up to 2%. Image distortion moves the apparent location of surface features and only a design change can minimize them, and low imaging distortion commercial systems are available. Care must be taken to recognize the imaging distortion present.

The distortion due to reference spheres is an inherent error. This error is caused by mapping a spherical surface onto a flat detector; it is analogous to the cartography problem of an earth map projection. This error causes both location errors such as distortion in the imaging system and coma wavefront errors when tilt fringes are added to the cavity.

When measuring the form of spherical or flat parts image distortion is not a problem if the fringes are nulled. Image distortion is problematic when spot polishing correction is required or when aspheric parts are measured.

Spot polishing requires the position of a surface feature to be known to a fraction of the size of the spot polishing tool footprint. Distortion causes features to appear shifted from their physical location. If this distorted location is used to position a spot polishing tool the correction will occur in the wrong location creating greater errors. Each polishing tool footprint or work function must be considered to determine the acceptable distortion in the interferometer. In a 1-K×1-K imager system 0.1% distortion produces a 1-pixel error at the edge of the field, this is sufficient for most situations.

For aspheres, mapping the surface deviation from the spherical reference translates into height errors when the image is distorted. The asphere can be more or less curved in error depending on the shape and amount of image distortion. Also the mapping distortion caused by the reference sphere will add coma wavefront distortion where tilt fringes are observed. The amount of this error will depend on local slopes between the test and reference wavefronts and thus varies across the measured aspheric surface. Therefore, standard interferometers are not recommended for the measurement of aspheres and specialized systems are required as discussed in section 3.

5. Summary

In the introduction to Part 1 it was noted that an ideal interferometer would map the three-dimensional optical surface with no distortion (error) in height or position, regardless of whether the surface is a flat, sphere or asphere, be robust against environmental influences, and never produce an error. Numerous deviations from the ideal were noted in this paper with strategies to approach the ideal in actual practice. An awareness of these error sources and the target performance requirements plus the ability to measure and minimize their affects will lead to more consistent and higher quality metrology results.

In part 3, some advanced techniques to minimize systematic errors, plus data acquisition software and future trends will be discussed.

References

- [1] R. A. Smythe, *Adv. Opt. Technol.* 1 (2012).
- [2] R. A. Smythe, *op. cit.*
- [3] E. P. Goodwin and J. C. Wyant, in 'Field Guide to Interferometric Testing', Vol. FG10 (SPIE, 2006).
- [4] D. Malacara, Ed., in 'Optical Shop Testing' (John Wiley & Sons, Inc., Hoboken, NJ, USA, 2007) pp. 27–33.
- [5] L. L. Deck, P. J. DeGroot and J. A. Soobitsky, *SPIE Opti Fab.* (2011).
- [6] C. Ai, US Patent Office 5,452,088 (1995).
- [7] Y. Bitou and N. Ueki, *Meas. Sci. Technol.* 21.
- [8] K. Freischlad, US Patent 5,737,081 (1998).
- [9] Y. Dai, S. Chen, S. Li, H. Hu and Q. Zhang, *Optical Eng.* 50, 013601 (2011).
- [10] R. Donker, I. Widdershoven and H. Spaan, in 'Proc. Asian Symp. Precision Eng. Nanotechnol.' (2009).
- [11] K. Kubo, in '5th High Level Expert Meeting 2012 Asphere Metrology' (PTB, 2012).
- [12] J. Wyant and V. Bennett, *Appl. Opt.* 11, 2833–2839 (1972).
- [13] T. Köhle, in '5th High Level Expert Meeting 2012 Asphere Metrology' (PTB, 2012).
- [14] M. Kuechel, in *Frontiers in Optics, OSA Technical Digest (CD)* (Optical Society of America, 2006), paper OFTuB5.
- [15] J. E. Greivenkamp, *Appl. Opt.* 26, 5245–5258 (1987).
- [16] P. E. Murphy, G. Forbes and A. Kulawiec, in *Optical Fabrication and Testing, OSA Technical Digest (CD)* (Optical Society of America, 2010), paper OMA8.

- [17] M. F. Küchel, *SPIE Proc.* 7389 (2009).
- [18] R. Smythe, *Laser Focus World*, October (2006).
- [19] P. Szwaykowski and A. Olszak, in *Optical Fabrication and Testing*, OSA Technical Digest (CD) (Optical Society of America, 2010).
- [20] D. A. Pearson II, in '5th High Level Expert Meeting 2012 Asphere Metrology' (PTB, 2012).
- [21] J. H. Bruning, D. R. Herriot, J. E. Gallagher, D. P. Rosenfeld, A. D. White et al., *Appl. Opt.* 13 (1974).
- [22] J. A. Soobitsky, US Patent Office 4,577,131 (1986).
- [23] J. B. Hayes, US Patent Office 4,884,003 (1989).
- [24] R. Crane, *Appl. Opt.* 8, 538 (1969).
- [25] A. V. Zvyagin and D. D. Sampson, *Opt. Lett.* 26 (2001).
- [26] P. Dumas, D. Golini and M. Tricard, in 'American Society for Precision Engineering 19th Annual Meeting' (2004).
- [27] D. Malacara, Ed., in 'Optical Shop Testing' (John Wiley & Sons, Inc., 2007) pp. 595.
- [28] L. L. Deck, *Appl. Opt.* 48 (2009).
- [29] R. A. Smythe and R. C. Moore, *Opt. Eng.* 23 (1984).
- [30] M. Novak, J. Millerd, N. Brock, M. North-Morris, J. Hayes, et al., *Appl. Opt.* 44 (2005).
- [31] P. Szwaykowski, F. N. Bushroo and R. J. Castonguay, US Patent Office 8,004,687 (2011).
- [32] M. F. Küchel, US Patent Office 4,872,755 (1989).
- [33] B. Kimbrough, J. Millerd, J. Wyant and J. Hayes, *Proc. SPIE* 6292 (2006).
- [34] C. L. Koliopoulos, *Proc. SPIE* 1531, 119 (1992).
- [35] J. E. Millerd, N. J. Brock, J. Hayes, B. Kimbrough, M. Novak, et al., *Proc. SPIE* 5531, 304 (2004).
- [36] B. Kimbrough and J. Millerd, *Proc. SPIE* 7790, 77900K (2010).
- [37] M. Küchel, US Patent Office 5,361,312. (1994).
- [38] M. Takeda, H. Ina and S. Kobayashi, *J. Opt. Soc. Am.* 72, 156 (1982).
- [39] D. M. Sykora and P. de Groot, *Proc. SPIE* 8126, 812610 (2011).
- [40] 'International Vocabulary of Basic and General Terms in Metrology' (International Organization for Standardization, 1993), section 3.9.
- [41] 'International Vocabulary of Basic and General Terms in Metrology', (International Organization for Standardization, 1993), section 2.6.
- [42] 'Acceptance and Rejection Zone in Decision Rules', ASME B89.7.3.1, section 4 (2001).
- [43] U. Griesmann, Q. Wang, J. Soons and R. Carakos, *Proc. SPIE* 5869, 58690S (2005).
- [44] B. S. Fritz, *Proc. SPIE* 433, 123 (1983).
- [45] G. Schulz and J. Schwider, *Opt. Eng.* 26, 559 (1987).
- [46] E. Jensen, *J. Opt. Soc. Am.* 63, 1313A (1973).
- [47] F. Morin and S. Bouillet, *Proc. SPIE* 6616, 66164G (2007).
- [48] M. F. Küchel, *Optik (Jena)* 112, 381–391 (2001).
- [49] U. Griesmann, Q. Wang and J. Soons, *Opt. Eng.* 46, 093601 (2007).
- [50] M. F. Küchel, *Proc. SPIE* 7389 (2009).
- [51] J. Biegen, US Patent Office 4,820,049 (1989).
- [52] L. L. Deck, US Patent Office 6,924,898 (2005).



Robert Smythe has over 30 years experience in the field of interferometry. Beginning at Corning Tropol he developed displacement measuring interferometers and interferometers to measure glass homogeneity and surface figure. He then moved to Zygo Corporation and for over 20 years created interferometer-based products to measure surface finish, waviness and form for markets ranging

from semiconductor lithography optical systems to automotive engine components. In addition to development engineering, Robert also led marketing and sales at Zygo gaining insight into the practical application of interferometers in diverse applications. He now operates a consulting business aimed at product creation, development and application, and global marketing of high technology products, primarily optical based metrology systems.